

Defect-controlled densification and negative thermal expansion in UiO-66(Hf)

Electronic Supporting Information

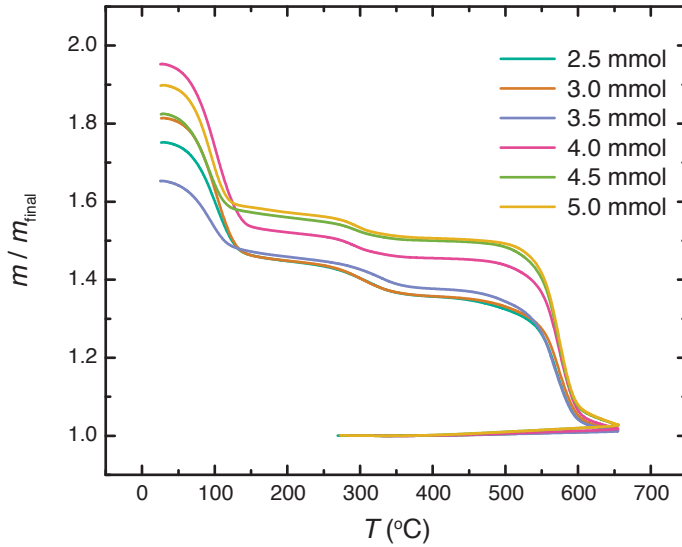
Matthew J. Cliffe, Joshua A. Hill, Claire A. Murray,
François-Xavier Coudert and Andrew L. Goodwin*

March 5, 2015

Department of Chemistry, University of Oxford,

Inorganic Chemistry Laboratory, South Parks Road, Oxford OX1 3QR, U.K.

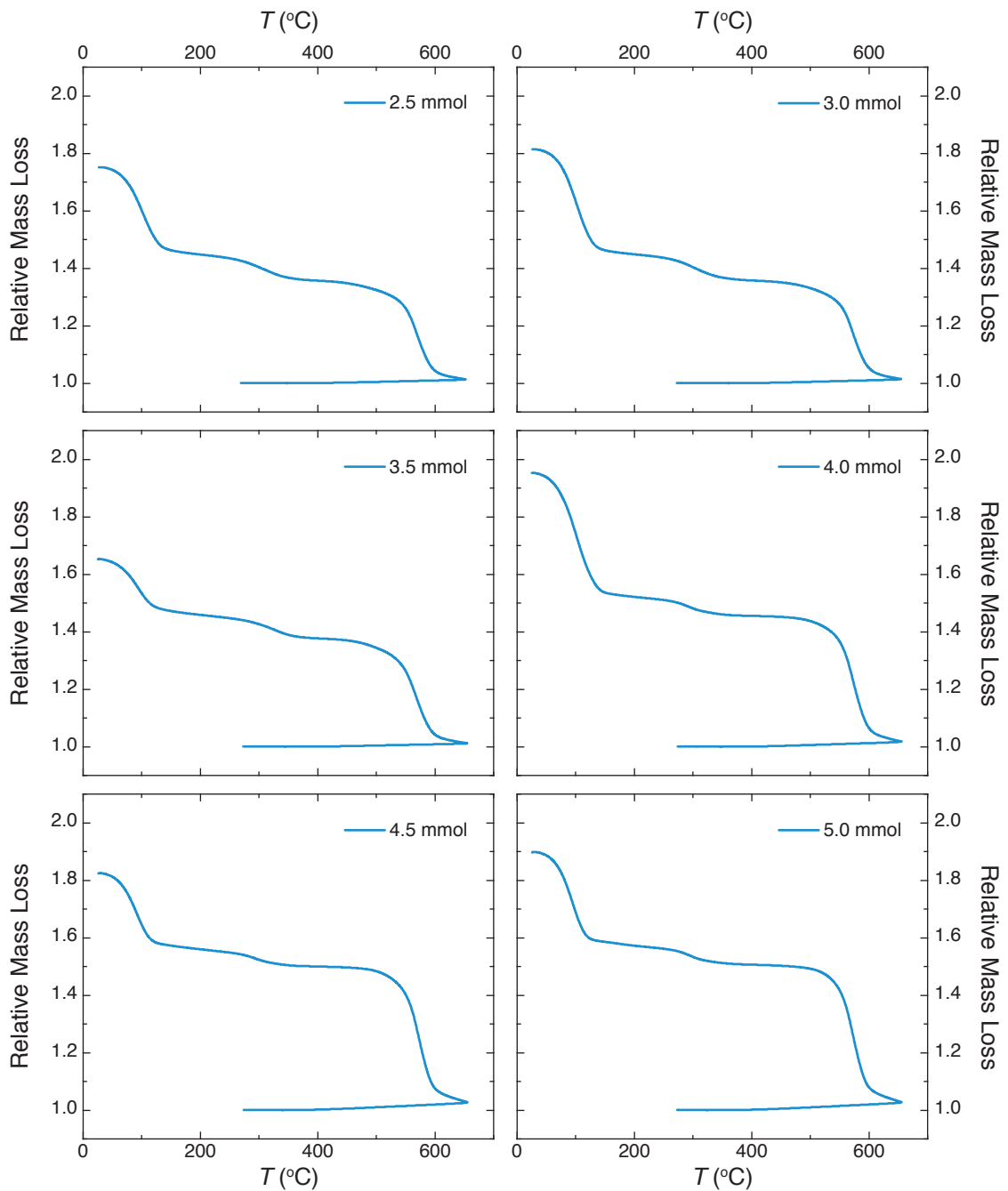
*To whom correspondence should be addressed; e-mail: andrew.goodwin@chem.ox.ac.uk.



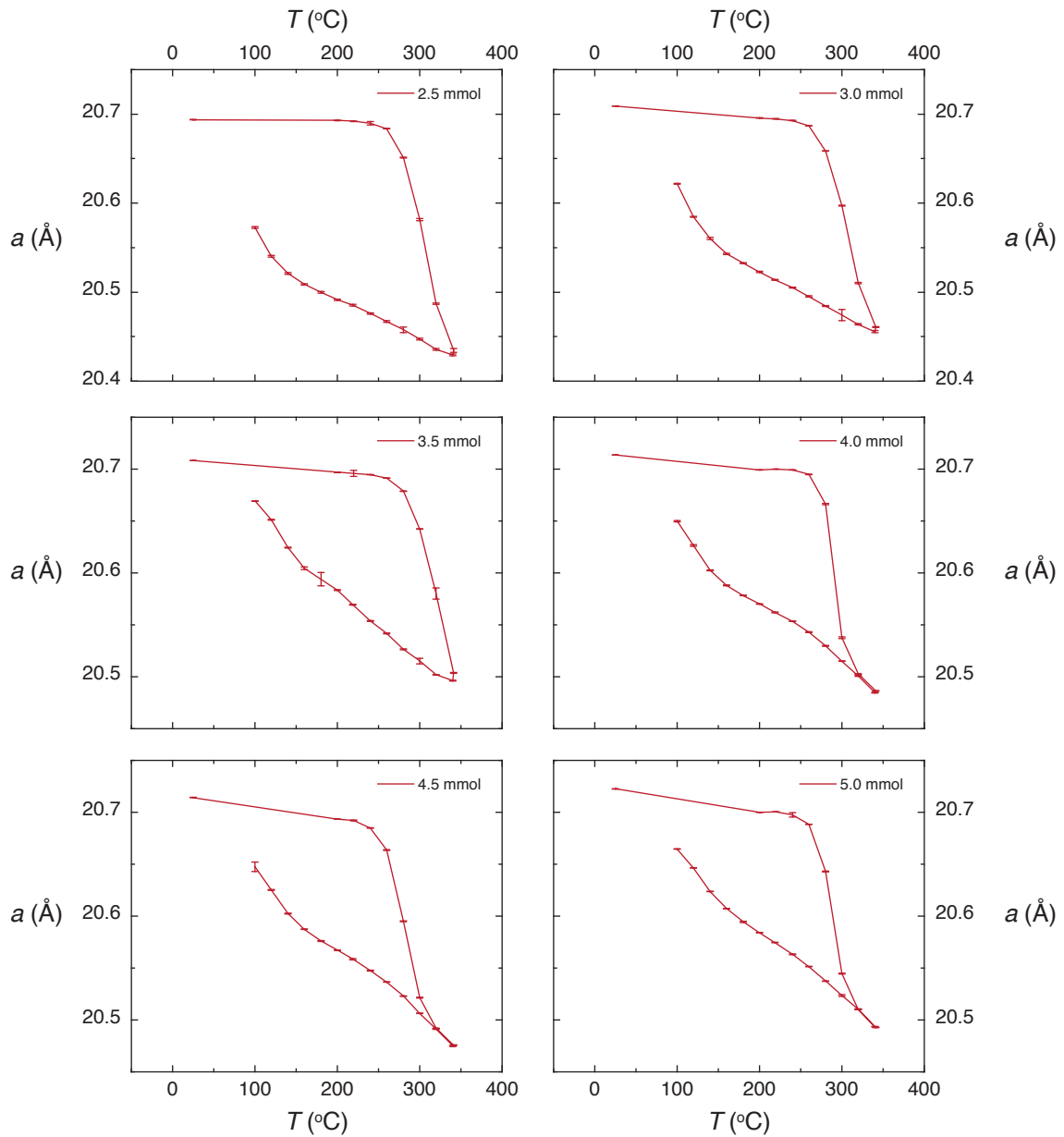
ESI Fig. 1: TGA measurements of defective UiO-66(Hf), summarised in Fig. 2(c,d) of the main text. All masses have been scaled to the lowest mass. Three steps, corresponding to desolvation, ligand elimination and decomposition are clearly visible in all samples.

n BDC (mmol)	$I(110) / I(111)$	$a_{200^\circ\text{C}} / a_{380^\circ\text{C}} - 1$ (%)	$\alpha_a (\text{MK}^{-1})$
2.5	0.163(3)	1.843(12)	-23.4(8)
3	0.136(3)	1.381(5)	-26.9(1.3)
3.5	0.099(3)	1.178(7)	-31.6(7)
4	0.055(3)	1.089(2)	-29.3(1.8)
4.5	0.036(3)	0.964(5)	-31.2(1.5)
5	0.026(5)	0.946(6)	-32.4(1.3)

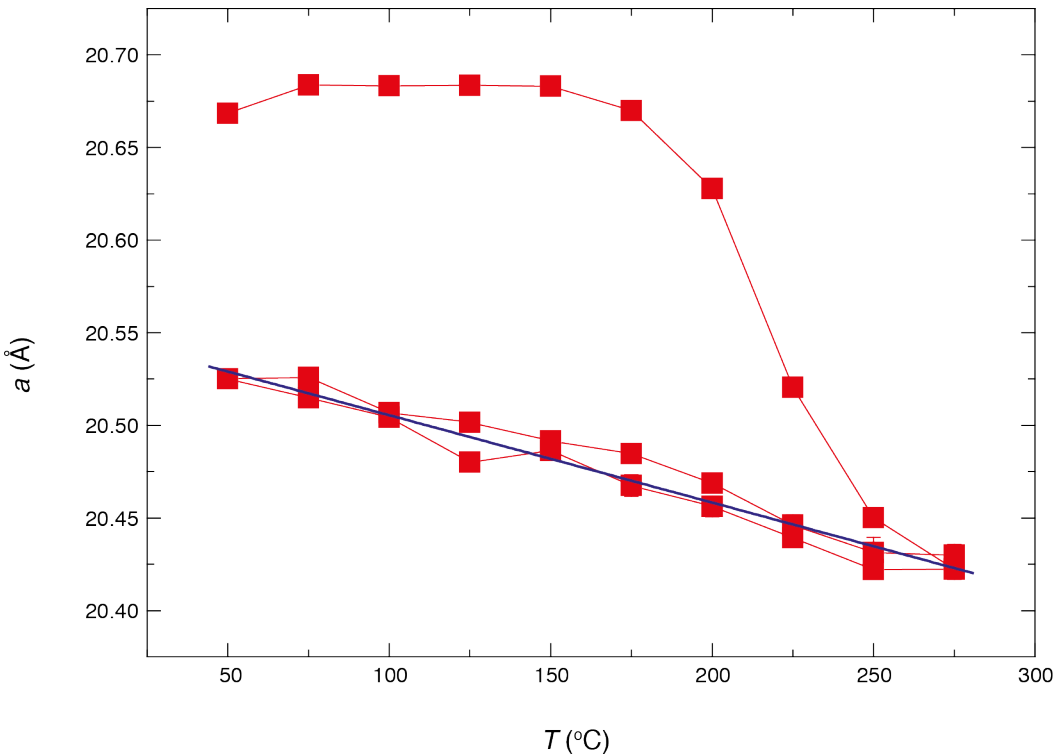
ESI Table 1: Summary of the data presented in Fig. 4 of the main text.



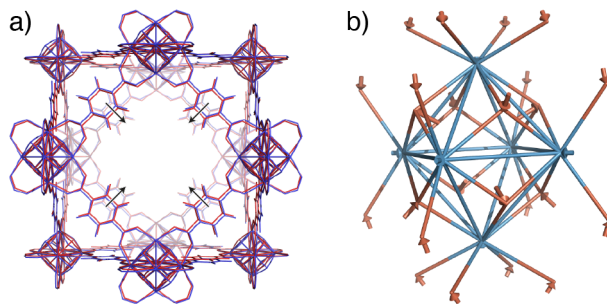
ESI Fig. 2: TGA measurements of defective UiO-66(Hf). The data are displayed separately here for clarity.



ESI Fig. 3: Synchrotron PXRD diffraction measurements of the variation in lattice parameter for defective UiO-66(Hf), on heating from 200–340 °C followed by cooling to 100 °C. These measurements were used to calculate the values shown in Fig. 4(c,d) in the main text.



ESI Fig. 4: Laboratory PXRD diffraction measurements of the variation in lattice parameter for defective UiO-66(Hf) (synthesised with 2.5 mmol of H₂bdc), on heating from 50–275 °C, cooling to 50 °C and then heating to 275 °C again, under flow of N₂ gas, demonstrating the reversibility of the NTE. A linear fit to the lattice parameter (shown in blue) to lattice parameter for the cooling and second heating (275–50–275 °C) yields $\alpha_V = -69(4) \text{ MK}^{-1}$. Errors contained within points unless shown. Measurements were made on a Siemens D5000 diffractometer in Bragg Brentano geometry using Cu K α radiation, equipped with an Anton Paar furnace, measured over the angular range $2\theta = 5\text{--}60^\circ$.



ESI Fig. 5: The structural changes found on relaxing the ligand-eliminated **reo** UiO-66(Hf). On a unit cell level, (a), the most obvious change between the initial (blue) to the final, post-ligand loss, (red) structures is a translation of the BDC linkers relative to the metal cluster edges. This results from the local changes in the cluster shown in panel (b). In particular the reduction in the equatorial Hf coordination number from eight to six both causes a substantial volume contraction of the cluster itself and leads to the previous symmetric binding of the remaining BDC linkers to become asymmetric. This is responsible for observed shift in the positions of the BDC ligands. The cluster after modulator elimination is shown, with displacements in the atoms indicated by arrows (the lengths of the arrows are double the actual displacements, so they can be more easily seen).

<i>n</i> (BDC) (mmol)	2.5		3.0		3.5		4.0		4.5		5.0		
T(°C)	a (Å)	error	T(°C)	a (Å)	error								
100	20.6981	0.0002	25	20.7047	0.0004	20.6942	0.0001	20.7131	0.0001	20.7026	0.0007	20.7165	0.0003
100	20.6983	0.0003	200	20.7019	0.0003	20.7040	0.0001	20.7075	0.0001	20.6945	0.0002	20.7251	0.0007
120	20.6974	0.0002	220	20.7012	0.0002	20.7031	0.0002	20.7077	0.0001	20.6936	0.0003	20.7218	0.0015
140	20.6972	0.0002	240	20.6987	0.0002	20.7020	0.0001	20.7044	0.0004	20.6887	0.0003	20.7072	0.0017
160	20.6963	0.0002	260	20.6923	0.0002	20.6988	0.0001	20.6907	0.0002	20.6770	0.0003	20.6880	0.0022
180	20.6950	0.0002	280	20.6740	0.0002	20.6891	0.0002	20.6288	0.0007	20.6472	0.0034	20.6504	0.0025
200	20.6940	0.0002	300	20.6241	0.0004	20.6612	0.0003	20.5410	0.0003	20.5848	0.0004	20.6096	0.0025
220	20.6913	0.0006	320	20.5519	0.0006	20.6106	0.0003	20.5114	0.0003	20.5380	0.0003	20.5782	0.0025
240	20.6885	0.0003	340	20.4786	0.0002	20.5197	0.0003	20.4924	0.0001	20.5122	0.0004	20.5549	0.0025
260	20.6828	0.0001	360	20.4449	0.0003	20.4892	0.0003	20.4812	0.0003	20.4995	0.0004	20.5313	0.0019
280	20.6689	0.0011	380	20.4242	0.0009	20.4726	0.0018	20.4772	0.0003	20.4911	0.0004	20.5249	0.0019
300	20.6369	0.0005	400	20.4063	0.0010	20.4593	0.0022	20.4711	0.0018	20.4795	0.0019	20.5220	0.0018
320	20.5530	0.0014	420	20.3814	0.0010	20.4496	0.0005	20.4706	0.0002	20.4767	0.0010	20.5198	0.0018
340	20.4342	0.0010	440	20.3639	0.0013	20.4435	0.0005	20.4717	0.0005	20.4740	0.0004	20.5209	0.0024
360	20.3822	0.0011	460	20.3414	0.0013	20.4407	0.0009	20.4711	0.0016	20.4745	0.0004	20.5249	0.0030
380	20.3431	0.0013	480	20.3261	0.0022	20.4368	0.0011	20.4697	0.0021	20.4732	0.0005	20.5374	0.0048
400	20.3094	0.0016	500	20.3236	0.0062	20.4194	0.0029	20.4730	0.0010	20.4705	0.0008	20.5289	0.0135

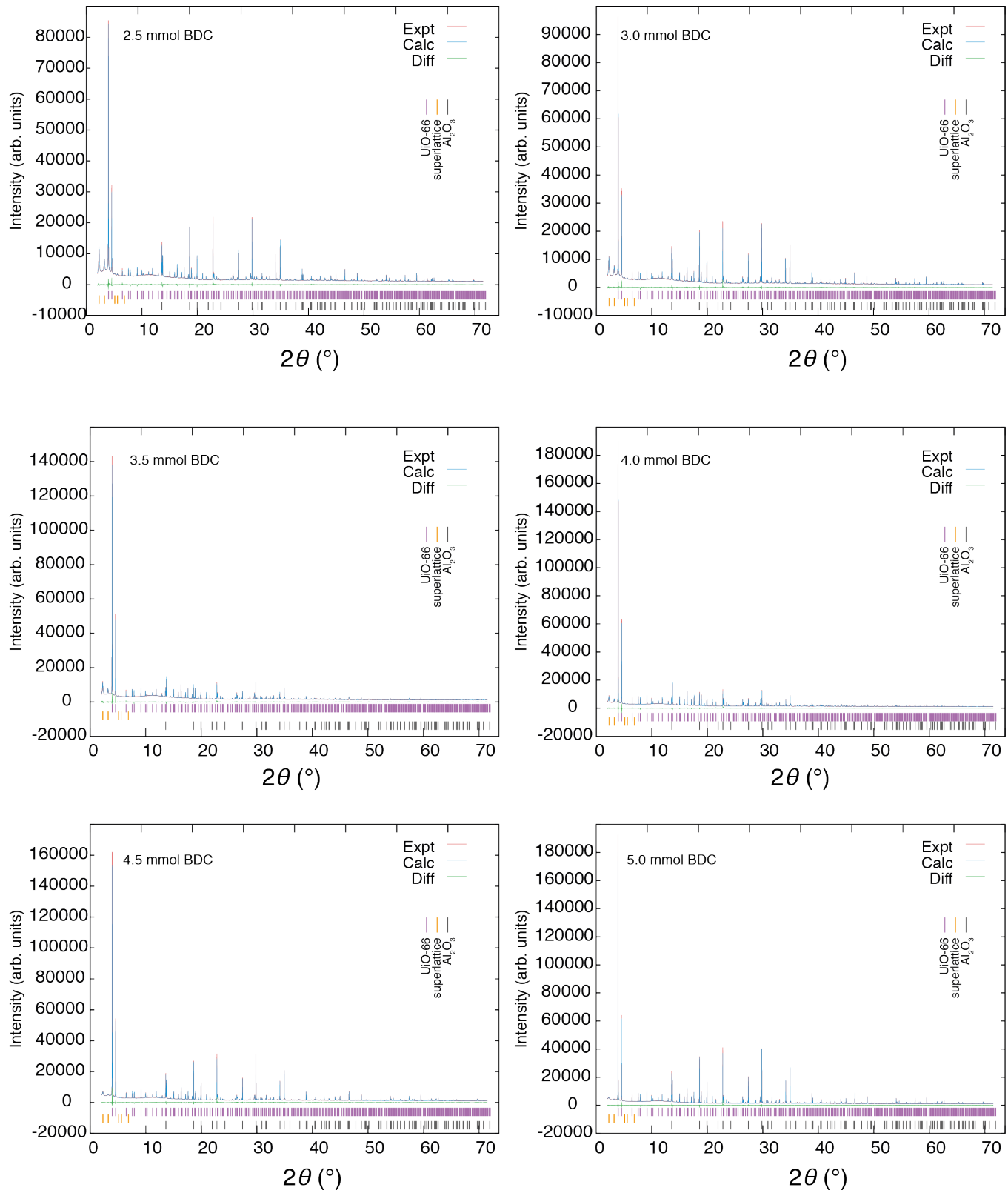
ESI Table 2: Lattice parameters, derived from Pawley fitting, for the initial variable temperature measurements used for the determination of densification, shown in Fig. 4(a,b) of the main text.

<i>n</i> (BDC) (mmol)	2.5	3.0	3.5	4.0	4.5	5.0						
T(°C)	a (Å)	error										
25	20.6937	0.0002	20.7090	0.0002	20.7082	0.0001	20.7136	0.0000	20.7141	0.0003	20.7226	0.0001
200	20.6930	0.0002	20.6957	0.0002	20.6970	0.0001	20.6991	0.0001	20.6935	0.0001	20.7001	0.0001
220	20.6921	0.0002	20.6947	0.0002	20.6958	0.0031	20.7000	0.0000	20.6921	0.0004	20.7005	0.0001
240	20.6897	0.0018	20.6928	0.0002	20.6946	0.0001	20.6992	0.0001	20.6848	0.0001	20.6975	0.0021
260	20.6835	0.0002	20.6869	0.0002	20.6913	0.0001	20.6948	0.0001	20.6636	0.0003	20.6883	0.0000
280	20.6513	0.0005	20.6585	0.0003	20.6787	0.0002	20.6662	0.0007	20.5953	0.1706	20.6429	0.0004
300	20.5815	0.0011	20.5972	0.0004	20.6423	0.0003	20.5375	0.0007	20.5215	0.0003	20.5447	0.0003
320	20.4870	0.0007	20.5102	0.0005	20.5804	0.0054	20.5028	0.0002	20.4921	0.0003	20.5101	0.0001
340	20.4345	0.0021	20.4607	0.0006	20.5039	0.0004	20.4864	0.0003	20.4758	0.0004	20.4928	0.0002
340	20.4294	0.0009	20.4557	0.0014	20.4961	0.0004	20.4848	0.0003	20.4751	0.0007	20.4934	0.0002
320	20.4355	0.0010	20.4637	0.0007	20.5020	0.0003	20.5009	0.0003	20.4913	0.0004	20.5102	0.0004
300	20.4474	0.0009	20.4743	0.0063	20.5151	0.0026	20.5150	0.0003	20.5064	0.0003	20.5236	0.0010
280	20.4577	0.0032	20.4845	0.0006	20.5266	0.0004	20.5297	0.0003	20.5229	0.0003	20.5375	0.0002
260	20.4671	0.0009	20.4952	0.0006	20.5418	0.0004	20.5429	0.0003	20.5365	0.0003	20.5513	0.0002
240	20.4759	0.0009	20.5052	0.0004	20.5537	0.0004	20.5535	0.0003	20.5476	0.0003	20.5634	0.0004
220	20.4853	0.0009	20.5137	0.0006	20.5693	0.0004	20.5619	0.0003	20.5586	0.0006	20.5745	0.0003
200	20.4916	0.0008	20.5226	0.0006	20.5836	0.3518	20.5701	0.0003	20.5672	0.0003	20.5840	0.0002
180	20.4999	0.0009	20.5325	0.0006	20.5938	0.0064	20.5782	0.0002	20.5760	0.0003	20.5945	0.0006
160	20.5087	0.0009	20.5430	0.0006	20.6044	0.0012	20.5879	0.0004	20.5873	0.0003	20.6073	0.0002
140	20.5209	0.0010	20.5602	0.0013	20.6242	0.0004	20.6025	0.0003	20.6026	0.0004	20.6236	0.0002
120	20.5404	0.0009	20.5846	0.0006	20.6514	0.0004	20.6264	0.0010	20.6252	0.1154	20.6464	0.0002
100	20.5726	0.0009	20.6216	0.0006	20.6693	0.0003	20.6499	0.0006	20.6474	0.0045	20.6646	0.0003

ESI Table 3: Lattice parameters, derived from Pawley fitting, for the final variable temperature measurements used for determination of the coefficients of NTE shown in Fig. 4(c,d) of the main text. These data are displayed in ESI Fig. 5.

$n(\text{BDC})$ mmol	R_{wp}	$a (\text{\AA})$	σ	Hf x	σ	Hf U_{iso} (\AA^{-2})	σ	non-Hf U_{iso} (\AA^{-2})	σ
2.5	3.004	20.69023	0.00009	0.11953	0.00005	0.02434	0.0002	0.074	0.002
3.0	2.976	20.69383	0.00008	0.11958	0.00005	0.02197	0.0002	0.064	0.002
3.5	3.122	20.69589	0.00007	0.11954	0.00004	0.019265	0.00016	0.0630	0.0016
4.0	3.340	20.69789	0.00006	0.11953	0.00003	0.017477	0.00013	0.0502	0.0013
4.5	3.477	20.69164	0.00008	0.11954	0.00004	0.022260	0.00019	0.0523	0.0016
5.0	3.446	20.69926	0.00005	0.11944	0.00004	0.017085	0.00014	0.0458	0.0013

ESI Table 4: Refined parameters for the Rietveld fits shown in ESI Fig. 6.



ESI Fig. 6: Rietveld fits for each sample at 200 °C. The data were fit with three phases: **fcu**-UIO-66(Hf), Al_2O_3 and a Pawley phase accounting for the broad superlattice reflections, using the same cell parameter as for the UIO-66(Hf) Rietveld phase.